

See discussions, stats, and author profiles for this publication at: <https://www.researchgate.net/publication/41434352>

Diverted Total Synthesis Leads to the Generation of Promising Cell-Migration Inhibitors for Treatment of Tumor Metastasis: In vivo and Mechanistic Studies on the Migrastatin Core E...

ARTICLE *in* JOURNAL OF THE AMERICAN CHEMICAL SOCIETY · FEBRUARY 2010

Impact Factor: 12.11 · DOI: 10.1021/ja9101503 · Source: PubMed

CITATIONS

41

READS

39

11 AUTHORS, INCLUDING:



Thordur Oskarsson

German Cancer Research Center

26 PUBLICATIONS 3,287 CITATIONS

SEE PROFILE



Guangli Yang

Memorial Sloan-Kettering Cancer Center

21 PUBLICATIONS 1,269 CITATIONS

SEE PROFILE



Ouathék Ouerfelli

Memorial Sloan-Kettering Cancer Center

44 PUBLICATIONS 2,502 CITATIONS

SEE PROFILE



Published in final edited form as:

J Am Chem Soc. 2010 March 10; 132(9): 3224–3228. doi:10.1021/ja9101503.

Diverted Total Synthesis Leads to the Generation of Promising Cell-Migration Inhibitors for Treatment of Tumor Metastasis: In vivo and Mechanistic Studies on the Migrastatin Core Ether Analog

Thordur Oskarsson[§], Pavel Nagorny[†], Isaac Krauss[†], Lucy Perez[†], Mihiribaran Mandal[†], Guangli Yang⁺, Ouathék Ouerfelli⁺, Danhua Xiao[#], Malcolm Moore[#], Joan Massagué^{§, ^}, and Samuel J. Danishefsky^{†, ‡}

Samuel J. Danishefsky: s-danishefsky@ski.mskcc.org

[§]Cancer Biology and Genetics Program, Memorial Sloan-Kettering Cancer Center, 1275 York Avenue, New York, NY 10065

[#]Cell Biology Program, Memorial Sloan-Kettering Cancer Center, 1275 York Avenue, New York, NY 10065

[†]Laboratory for Bioorganic Chemistry, Memorial Sloan-Kettering Cancer Center, 1275 York Avenue, New York, NY 10065

⁺Organic Synthesis Core Facility, Memorial Sloan-Kettering Cancer Center, 1275 York Avenue, New York, NY 10065

[^]Howard Hughes Medical Institute, Memorial Sloan-Kettering Cancer Center, 1275 York Avenue, New York, NY 10065

[‡]Department of Chemistry, Columbia University, Havemeyer Hall, 3000 Broadway, New York, NY 10027

Abstract

A significantly simpler analog of the natural product migrastatin, termed migrastatin ether (ME), has been prepared and evaluated. Both *in vivo* and *in vitro* studies indicate that ME exhibits a concentration-dependent inhibitory effect on migration of breast cancer cells.

Introduction

Despite extensive research directed to the prevention, detection, and treatment of various cancers, one of the important factors regarding the high mortality rate of various tumors is the phenomenon of tumor metastasis.¹ Much remains to be accomplished in finding new strategies for dealing with the immense problem of metastasis. Such efforts are well justified since success in this regard could play a major role in reducing the ravages of cancer. We describe the discovery of a promising cancer cell migration inhibitor, **2**, which could have significant potential for attenuating the progression of metastasis.

Correspondence to: Samuel J. Danishefsky, s-danishefsky@ski.mskcc.org.

Supporting Information. Experimental procedures, copies of spectral data, and characterization (PDF). This material is available free of charge *via* the Internet at <http://pubs.acs.org>.

The starting point for this investigation was the reported isolation of a new polyketide natural product from *Streptomyces* sp. MK929-43F1 by Imoto and coworkers.² Shortly afterwards, it was recognized that this product is a migration inhibitor of cancer cells with IC₅₀s in μ M range. Accordingly, the natural product was named migrastatin (**1**). This initial report prompted us, as well as others, to pursue the total synthesis of migrastatin. In addition to the interesting chemistry level issues associated with such a goal, we were also motivated by the aim of preparing simplified and more potent cancer cell migration inhibitors using the logic of diverted total synthesis.³ Indeed, our group reported the inaugural total synthesis and the *in vitro* biological evaluation of **1** as well as several fully synthetic analogs (Figure 1).⁴

Remarkably, it was discovered in the context of those studies that *deletion of the entire glutarimide sidechain, as well as the α,β -unsaturated lactone moieties, from the migrastatin-like structure did not abrogate inhibition of cell migration*. Indeed, the “*des-side chain*” compounds are in some cases strikingly (10^3) more potent than is **1**.⁴ Based on this study, we selected several even more deeply simplified analogs of **1**: migrastatin core ether (**2**, ME), migrastatin core lactam (**3**) and migrastatin core ketone (**4**, MK) for further evaluation. Although both **3** and **4** have shown promising results in their ability to selectively inhibit cancer cell migration both *in vitro* and *in vivo*,⁴ the simplicity of structure **2** makes it a particularly attractive candidate for potential development. In this study, we describe the total synthesis and *in vivo* biological evaluation of migrastatin analog **2**, as demonstrated in mouse models. As will be shown herein, compound **2** exhibits promising properties which could well be exploited for the suppression of metastasis.

In synthesizing analog **2**, we built upon the findings of our total synthesis of migrastatin itself (**1**).^{3a,b} The assembly of **2** commenced from the known starting material **6**, prepared in three steps from commercially available 2,3-*O*-isopropylidene-1-tartrate **5** (Scheme 1).^{3a,5} Chelation-controlled Lewis acid-catalyzed diene aldehyde cyclocondensation (LACDAC) of **6** with diene **10**⁶ led to enone **7** in 87% yield as the single diastereomer.⁷ With the three contiguous stereocenters thus established, the installation of the trisubstituted (*Z*)-alkene by a reduction/Ferrier rearrangement sequence was addressed. Thus, the reduction of **7**⁸ followed by treatment of the resultant allylic alcohol with aqueous CSA, provided lactol **8**⁹ which was reduced with LiBH₄, thereby providing the corresponding diol in 73% yield from **7**. The latter was converted to allylic bromide **9** by a 2-step sequence (77% yield) involving selective bromination of the primary alcohol¹⁰ followed by protection of the secondary alcohol as a *t*-butyldimethylsilyl (TBS) ether. The reactive allylic bromide was etherified with compound **11** (90% yield),¹¹ and the resulting product was cyclized with the 2nd generation Grubbs catalyst.¹² Deprotection of the RCM product with HF·Py provided macrocycle **2** (68%, 2 steps).

Results and Discussion

In the wake of this efficient synthesis of **2** came the opportunity to study its effect on biological processes. We first evaluated the effect of ME (**2**) on cell migration in the human breast cancer cell lines MDA-MB-231 (hereafter called MDA231) and MDA-MB-435, using *in vitro* wound-healing assay. In one instance, we evaluated, *in vitro*, the relative potencies of ME (**2**) relative to the previously reported MK (**4**).¹³ ME (**2**) at 10 μ M almost completely inhibited the migration of both cell lines induced by serum (data not shown). We then tested the compound in the transwell cell-migration assay where the compound inhibited 4T1 cells, MDA231 and MDA-MB-435 cell migration with IC₅₀ in the range from 0.30 – 0.47 μ M (Table 1). Interestingly, a \sim 1,000-fold higher concentration of ME (**2**) was required for comparable inhibition of normal human mammary epithelial MCF10A cells (IC₅₀ 408 μ M). In contrast to the potent inhibitory effect on MDA231 cell migration, ME (**2**) did not have a comparable effect on cell proliferation, IC₅₀ 550 μ M (data not shown). This suggests that the major

biological effect of this compound (**2**) is inhibition of cell migration rather than inhibition of cell proliferation.

In the light of these results, we administered the compound (**2**) to the highly metastatic breast cancer cell line LM2-4175 (hereafter called LM2). LM2 cells are highly aggressive and metastatic derivatives of MDA231 cells with increased propensity to form lung metastasis.¹⁴ In vitro transwell assays were done where LM2 cells were pre-incubated with incremental concentrations of ME (**2**) lasting 24 hours before the assay. Migration of LM2 cells was significantly inhibited at concentrations of 2.5 μ M and 5 μ M (Figure 2). Furthermore, comparison of inhibitory effects of the core ether analog ME (**2**) and migrastatin (**1**) showed that ME exhibited a superior inhibitory effect at 5 μ M concentration (Figure 3). Neither ME (**2**) nor migrastatin (**1**) affected the viability of LM2 cells at these concentrations (Supplemental Tables 1 and 2).

ME (**2**) Treatment in a Human Breast Cancer Xenograft Model Inhibited Tumor Invasion and Metastasis and Prolonged Overall Survival in NOD/SCID Mice

To assess the ability of ME (**2**) to inhibit tumor metastasis *in vivo*, we utilized luciferase-based noninvasive whole animal bioluminescent imaging in a xenograft breast cancer model in NOD/SCID mice transplanted with MDA231 cells stably expressing the HSV-TK-eGFP-luciferase (TGL) reporter protein.¹⁵ Mice were inoculated with 1×10^7 tumor cells in the abdominal mammary gland area, and groups of five mice were given ME (**2**) (40 mg/kg) i.p. 3 times per week beginning either at day 1, when the tumor cells were injected (ME (**2**)-pre group), or from day 15 when the primary tumors were surgically resected (ME (**2**)-post group). The control mice were treated with PBS. Tumor volume and distribution were measured by serial bioluminescent imaging (see Supplemental Figure 3). At the time of surgical resection, 50% of control mice had metastases and 85% had tumors invaded into the muscle layer and peritoneal membrane. ME (**2**)-pretreatment markedly localized the tumor to the original injection site. One week after resection, imaging showed extensive metastases in control mice, a 47% reduction in metastases in the ME (**2**)-post group and a significant 87% reduction in the ME (**2**)-pre group (Fig 4A). ME (**2**)-post treatment had little effect on overall survival, with mortality attributed to tumor growth at sites of metastasis established prior to ME (**2**) treatment and to recurrence of tumor at the resection site (Figure 5). The ME (**2**)-pre group showed significantly prolonged overall survival with mortality attributed to recurrence of tumor growth at the site of resection rather than in metastatic sites (Figure 5). This was confirmed by histopathological studies at 2 weeks post-resection showing in the control group a systemic carcinomatosis involving almost all visceral organs and tissues including liver, lung, spleen, pancreas, mesenteric lymph nodes, kidney, and multifocal bone marrow sites (data not shown). ME (**2**)-post treatment did not prevent systemic carcinomatosis, with the exception of bone marrow that, in contrast to the control mice, was not a site of metastasis. In marked contrast, in the ME (**2**)-pre group, carcinoma was confined to the tumor resection site in the mammary fat pad and there was no evidence of systemic carcinomatosis. There was no significant body-weight loss in the treatment groups compared with the control, indicating that at this dosage ME (**2**) was not toxic to the animals.

In a second study comparing two dose levels of ME (**2**), NOD/SCID mice were again injected in the abdominal mammary fat pad with 1×10^7 MDA231 cells. At day 1, groups of 8 mice were injected with low dose ME (**2**) (40mg/kg i.p. 3 \times weekly), high dose ME (**2**) (200mg/kg i.p. 3 \times weekly), or control PBS. After 4 weeks the primary tumors were surgically resected and bioimaging for metastatic tumor was undertaken weekly. One week after resection, imaging showed extensive metastases in control mice with a significant 88-93% reduction in metastases with both high and low dose ME (**2**) mice (Figure 4B). At 7 weeks, groups of mice were sacrificed and the lung, liver, spleen and thymus were surgically removed and imaged.

There was extensive detectable metastatic growth of tumor in lung and liver of control mice but none in the ME (**2**)-treated mice (Supplemental Figure 1). By 9 weeks there was detectable metastatic tumor in lung and liver in the 40mg ME (**2**) group but the 200mg high dose group had no detectable metastases at this time (Supplemental Figure 1). Within 50 days, all mice in the untreated control cohort had died. However, at this time point the survival within the ME treated cohorts was 30% for 40mg/kg and 50% for 200mg/kg treatment (Supplemental Figure 2).

In a separate cohort of experiments, the ability of migrastatin core ether (**2**) to prevent lung metastasis of LM2 cells was studied. As mentioned, LM2 cells are originally derived from the MDA231 cells and have increased metastatic efficiency of seeding in lungs.¹⁴ Taking advantage of an *in vivo* model with increased specificity, we set out to test the efficacy of ME as an inhibitor. To assay metastatic activity *in vivo*, LM2 cells were inoculated orthotopically in the mammary fat pad of immunodeficient NOD.SCID mice. Mammary tumors were monitored and allowed to grow for 27 days before initiation of treatment (Figure 6). Animals were treated three times per week with **2** (ME) at 100mg/kg or 200mg/kg dosage and lung metastasis was determined by *ex vivo* bioluminescence imaging at day 42. The average luminescence was reduced by 2.5-fold with 100 mg/kg treatment of **2** and 4.5-fold with 200 mg/kg treatment of **2** (Figure 6B), indicating significant reduction in lung metastatic burden. Despite relatively high variability within cohorts, suppression of lung metastasis was statistically significant ($P < 0.05$) in cohorts treated with 200 mg/kg. Interestingly, based on regular measurements of the mammary fat pad tumors, treatment with **2** did not significantly attenuate mammary tumor growth (Figure 6A), suggesting a selective effect on metastasis.

In order to assess the ability of **2** to inhibit the metastatic spread of cells that are already in circulation, a lung colonization assay based on inoculation of LM2 cells into the mouse venous system was performed. The treatment of the mice with **2** qualitatively exhibited a trend towards inhibition of metastatic outgrowth (Supplemental Figure 2). Five out of seven mice responded well but due to high variability within the cohort the effect did not achieve statistical significance. Together these results suggest that **2** can inhibit the migration of breast cancer cells *in vitro* and the dissemination of metastatic tumors *in vivo*.

Conclusion

In summary, a much simplified analog of migrastatin, termed migrastatin ether (**2**) been prepared and evaluated. Both *in vivo* and *in vitro* studies indicate that **2** exhibits a concentration-dependent inhibitory effect on migration of MDA231 and LM2 breast cancer cells. Treatment with **2** did not reduce the viability of either MDA231 or LM2 cells in culture, nor did such treatment suppress the rate of growth of MDA231 or LM2 cells as mammary tumors. However, treatment with ME (**2**) appeared to increase survival of mice injected with MDA231 breast cancer cells. Also, treatment with ME (**2**), initiated at the time of engraftment, profoundly suppressed metastasis at 7 weeks and at the highest dose used (200 mg/kg) there were no detectable metastases at 9 weeks (Supplemental Fig. 1). This did not translate into prolonged survival since tumor recurred in the mammary fat pad at the site of tumor resection, requiring sacrifice of the mice. Furthermore, delaying administration of ME (**2**) for 2 weeks after tumor engraftment did not prolong survival, presumably because metastasis to multiple sites had already occurred and ME did not suppress metastatic tumor development once metastatic tumor cells had seeded to multiple organs. These findings establish a specific effect on cellular migratory capabilities. Even at the highest doses used, ME was well tolerated, suggesting that it could be used in settings requiring chronic administration. The tumor line used was from a patient with metastatic tumor and it was thus not surprising that the subcutaneous tumor was releasing metastatic cells within the first two weeks of engraftment.

The data suggest possible clinical applications, for example, efficient resection of breast cancer at an early stage prior to release of metastatic cells, followed by chronic ME (**2**) treatment. A combination of ME (**2**) with drugs that suppress tumor growth at the primary or metastatic sites should also be evaluated and in this context we have shown third generation microtubule stabilizing epothilones such as fludelone and iso-fludelone to be highly effective against taxol-resistant breast tumors in xenograft models.¹⁶

Our findings establish a specific effect of ME (**2**) on tumor cellular migratory capabilities. Recently, we identified a set of 18 genes, whose expression in MDA231 and LM2 cells mediates lung metastatic activity.¹⁴ This lung metastasis signature (LMS) is associated with lung relapse in breast cancer patients.¹⁴ Most LMS genes encode secretory or cell surface proteins with the exception of Fascin-1, which is an actin-bundling protein implicated in cancer cell migration.¹⁷ A key role for Fascin-1 in MDA231 cell migration has recently been demonstrated.¹⁸ This evidence suggests that in MDA231 and LM2 cells ME interferes with a Fascin-1 dependent migratory behavior. Although there is still need for optimization at the level of formulation and potency,¹⁹ migrastatin macroether **2** already shows considerable promise as a specific inhibitor of cellular migration and has great potential for inhibiting metastatic dissemination.

We note in passing that the progression which led from migrastatin to compound **2** is very much in keeping with the discovery platform which we have termed diverted total synthesis (DTS).²⁰ In this modality, the achievements of total synthesis are channeled to provide access to otherwise inaccessible structural space built around high-pedigree structures such as small molecule natural products (SMNPs). Several other examples of the value of DTS for facilitating the discovery of very promising leads have been reported.²¹

Supplementary Material

Refer to Web version on PubMed Central for supplementary material.

Acknowledgments

This work was supported by NIH grants CA103823 (SJD), CA126518 (JM) and CA129243 (JM); by the Alan and Sandra Gerry Metastasis Research Initiative (JM); and by a Cancer Research Institute Gar Reichman Award (MM). JM is an Investigator of the Howard Hughes Medical Institute. PN thanks the National Institutes of Health for a Ruth L. Kirschstein postdoctoral fellowship (CA125934-02).

References

1. (a) Hedley BD, Winquist E, Chambers AF. *Expert Opin Ther Targets* 2004;8:527–536. [PubMed: 15584860] (b) Perez L, Danishefsky SJ. *ACS Chem Biol* 2007;2:159–162. [PubMed: 17373763]
2. (a) Nakae K, Yoshimoto Y, Sawa T, Homma Y, Hamada M, Takeuchi T, Imoto M. *J Antibiot* 2000;53:1130–1136. [PubMed: 11132958] (b) Nakae K, Yoshimoto Y, Ueda M, Sawa T, Takahashi Y, Naganawa H, Takeuchi T, Imoto M. *J Antibiot* 2000;53:1228–1230. [PubMed: 11132973] (c) Takemoto Y, Nakae K, Kawatani M, Tahahashi Y, Naganawa H, Imoto M. *J Antibiot* 2001;54:1104–1107. [PubMed: 11858668] (d) Nakamura H, Takahashi Y, Naganawa H, Nakae K, Imoto M, Shiro M, Matsumura K, Watanabe H, Kitahara T. *J Antibiot* 2002;55:442–444. [PubMed: 12061554]
3. (a) Gaul C, Danishefsky SJ. *Tetrahedron Lett* 2002;43:9039–9042. (b) Gaul C, Njardarson JT, Danishefsky SJ. *J Am Chem Soc* 2003;125:6042–6043. [PubMed: 12785819] (c) Reymond S, Cossy J. *Eur J Org Chem* 2006:4800–4804. (d) Reymond S, Cossy J. *Tetrahedron* 2007;63:5918–5929.
4. (a) Njardarson JT, Gaul C, Shan D, Huang XY, Danishefsky SJ. *J Am Chem Soc* 2004;126:1038–1040. [PubMed: 14746469] (b) Gaul C, Njardarson JT, Shan D, Dorn DC, Wu KD, Tong WP, Huang XY, Moore MAS, Danishefsky SJ. *J Am Chem Soc* 2004;126:11326–11337. [PubMed: 15355116] (c) Shan D, Chen L, Njardarson JT, Gaul C, Ma X, Danishefsky SJ, Huang XY. *PNAS* 2005;102:3772–3776. [PubMed: 15728385]

5. Lee WW, Chang S. *Tetrahedron: Asymmetry* 1999;10:4473–4475.
6. Danishefsky SJ, Yan CF, Singh RK, Gammill RB, McCurry PM Jr, Fritsch N, Clardy J. *J Am Chem Soc* 1979;101:7001–7008.
7. (a) Danishefsky SJ. *Aldrichimica Acta* 1986;19:59–68. (b) Danishefsky SJ. *Chemtracts* 1989;2:273–289. (c) Danishefsky SJ, Pearson WH, Harvey DF, Maring CJ, Springers JP. *J Am Chem Soc* 1985;107:1256–1268.
8. Luche JL, Gemal AL. *J Am Chem Soc* 1979;101:5848–5849.
9. Ferrier RJ. *J Chem Soc* 1964:5443–5449.
10. Appel R. *Angew Chem Int Ed Engl* 1975;14:801–811.
11. Inanaga J, Hirata K, Saeki H, Katsuki T, Yamaguchi M. *Bull Chem Soc Jpn* 1979;52:1989–1993.
12. Scholl M, Ding S, Lee CW, Grubbs RH. *Org Lett* 1999;1:953–956. [PubMed: 10823227]
13. The relative merits of compounds **2** and **4** as candidates for further development en route to the clinic are being evaluated. Toward that end, it will be necessary to conduct the extensive studies described herein on MK (**4**).
14. Minn AJ, Gupta GP, Siegel PM, Bos PD, Shu W, Giri DD, Viale A, Olshen AB, Gerald WL, Massagué J. *Nature* 2005;436:518–524. [PubMed: 16049480]
15. Minn AJ, Kang Y, Serganova I, Gupta GP, Giri DD, Doubrovin M, Ponomarev V, Gerald WL, Blasberg R, Massagué J. *J Clin Invest* 2005;115:44–55. [PubMed: 15630443]
16. Chou TC, Zhang X, Zhong ZY, Li Y, Feng L, Eng S, Myles DR, Johnson R Jr, Wu N, Yin YI, Wilson RM, Danishefsky SJ. *Proc Natl Acad Sci U S A* 2008;105:13157–13162. [PubMed: 18755900]
17. Hashimoto Y, Skacel M, Adams JC. *Int J Biochem Cell Biol* 2005;37:1787–1804. [PubMed: 16002322]
18. Kim MY, Oskarsson T, Acharyya S, Nguyen DX, Zhang XH, Norton L, Massagué J. *Cell* 2009;139:1315–1326. [PubMed: 20064377]
19. Hennenfent KL, Govindan R. *Annals of Oncology* 2006;17:735–749. [PubMed: 16364960]
20. Wilson R, Danishefsky SJ. *J Org Chem* 2006;71:8329–8351. [PubMed: 17064003]
21. (a) Rivkin A, Chou TC, Danishefsky SJ. *Angew Chem Int Ed* 2005;44:2838–2850. (b) Yun H, Chou TCh, Dong H, Tian Y, Li Y, Danishefsky SJ. *J Org Chem* 2005;70:10375–10380. [PubMed: 16323847] (c) Wright BJD, Hartung J, Peng F, Van de Water R, Liu H, Tan QH, Chou TC, Danishefsky SJ. *J Am Chem Soc* 2008;130:16786–16790. [PubMed: 19049469]

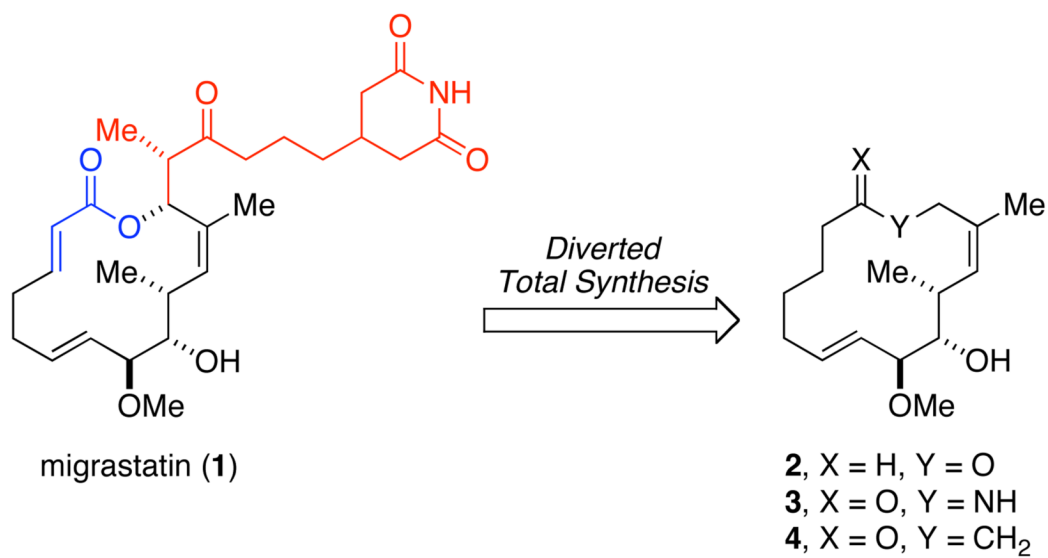


Figure 1.
Migrastatin and Synthetic Analogs.

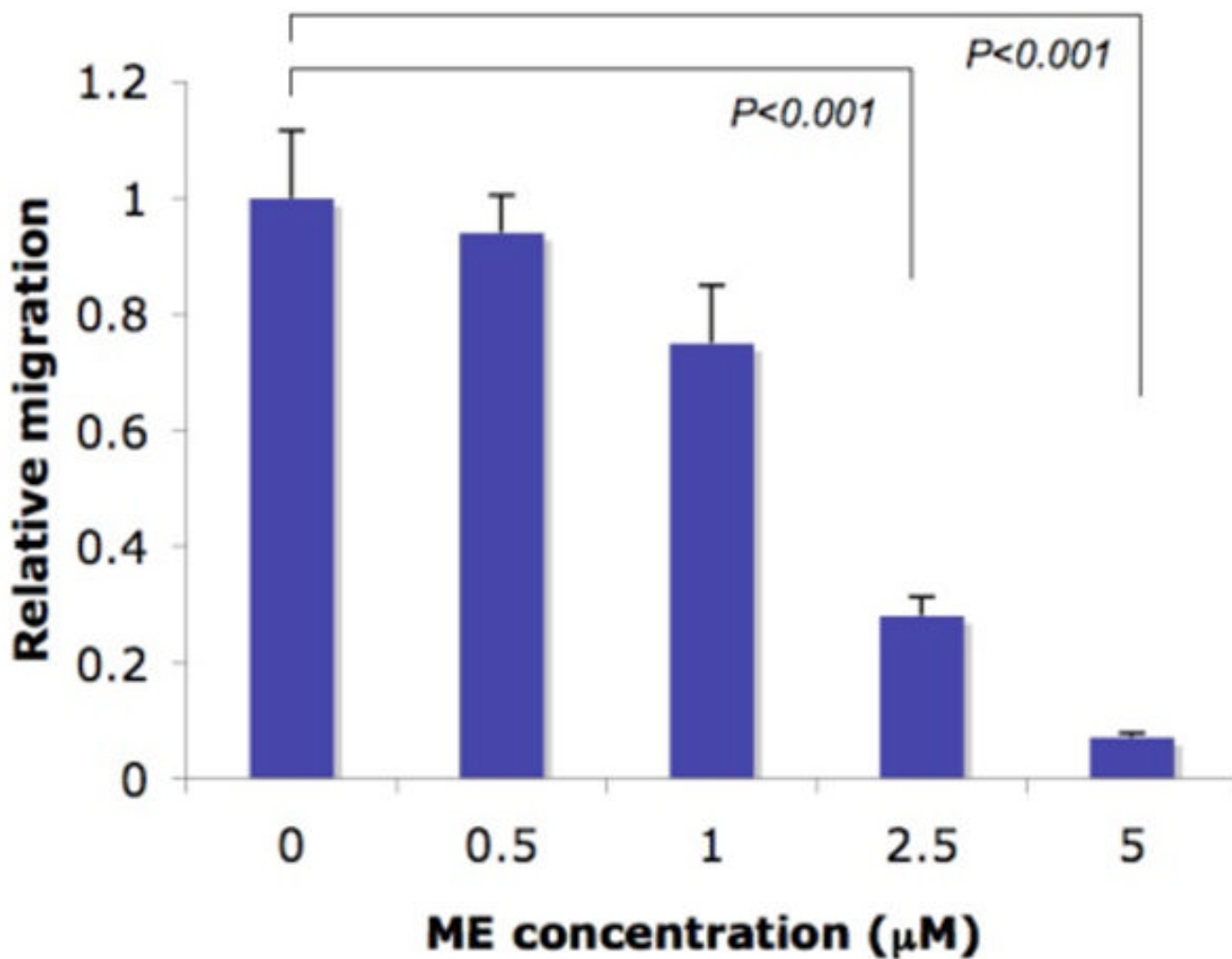


Figure 2.

ME mediated inhibition of LM2 cell migration. Transwell migration assay where LM2 cells were pre-treated for 24 hours with compound 2 (ME) at the indicated concentrations. P-values were determined using two-tailed Student's t-test.

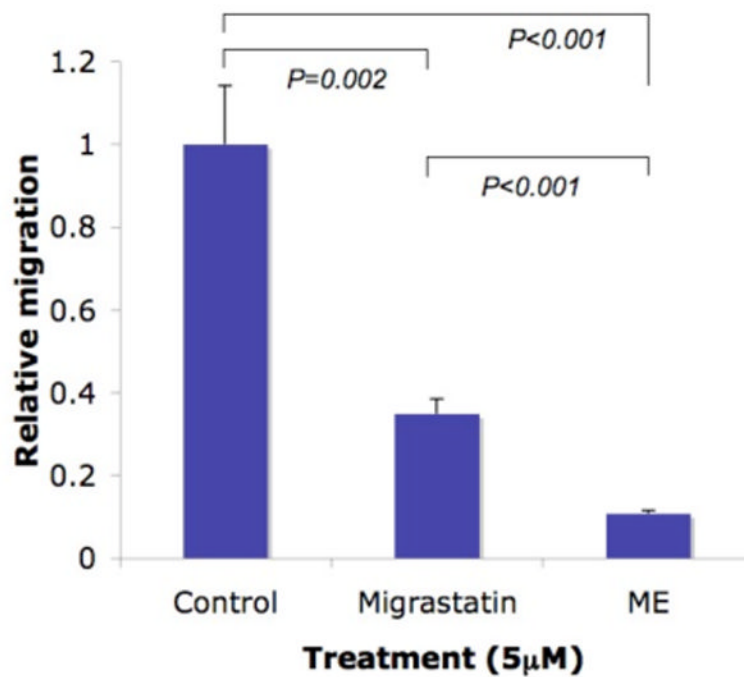
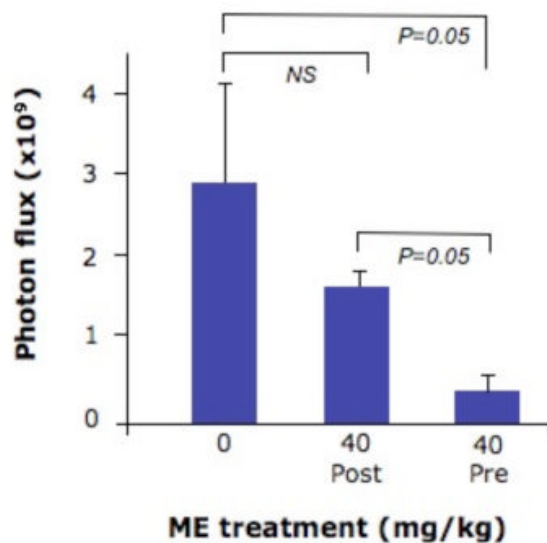
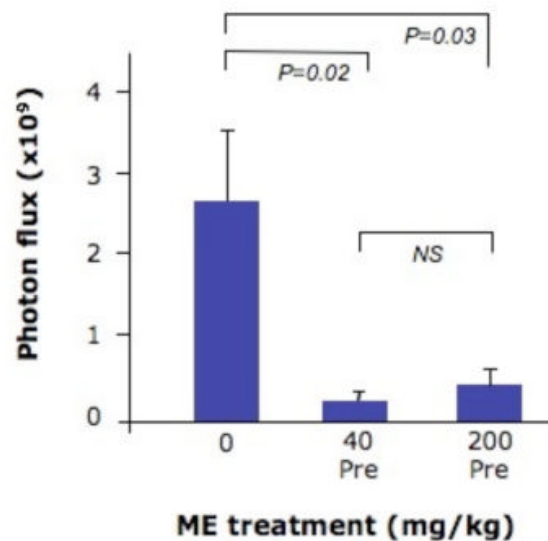


Figure 3.

Comparison of ME (2) and migrastatin (1) inhibitory activity. LM2 cells were pre-treated with 5μM ME or migrastatin and the migration ability was assessed with a transwell assay. P-values were obtained using two-tailed Student's t-test.

A.**B.****Figure 4.**

ME (2) inhibition of metastasis in mice inoculated with MDA231 cells as determined by bioimaging at one week after resection of primary tumor. MDA231 cells were injected into the mammary fat pad of NOD/SCID mice. The mice were treated with indicated dosages of ME (2), three times per week. **A.** ME (2) treatment (40 mg/kg) begun at day 1 or day 15 after tumor inoculation. Primary tumor was resected at 2 weeks and tumor metastasis determined by bioimaging at 3 weeks. **B.** ME (2) treatment (40 mg/kg or 200 mg/kg) begun at day 1 after tumor inoculation. Primary tumor was resected at 3 weeks and tumor metastasis determined by bioimaging at 4 weeks. P-values were obtained using two-tailed Student's t-test.

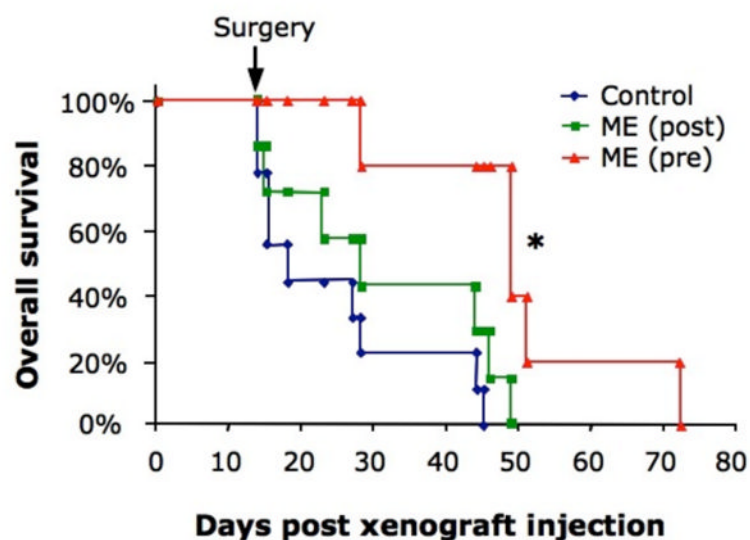
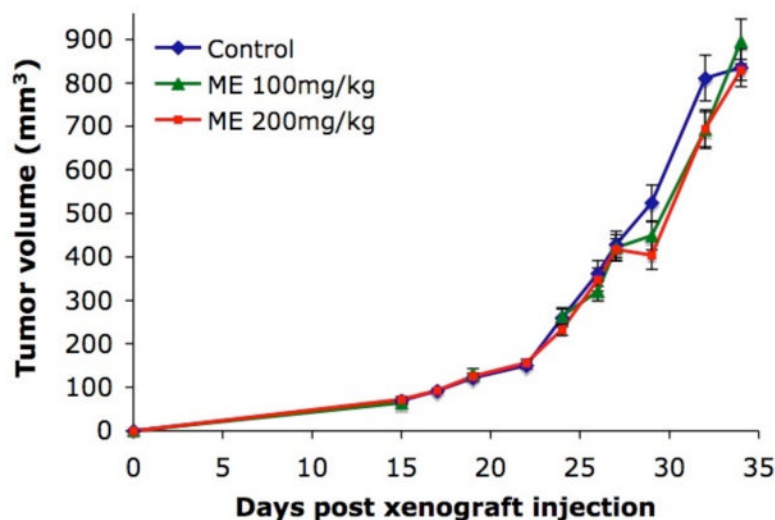


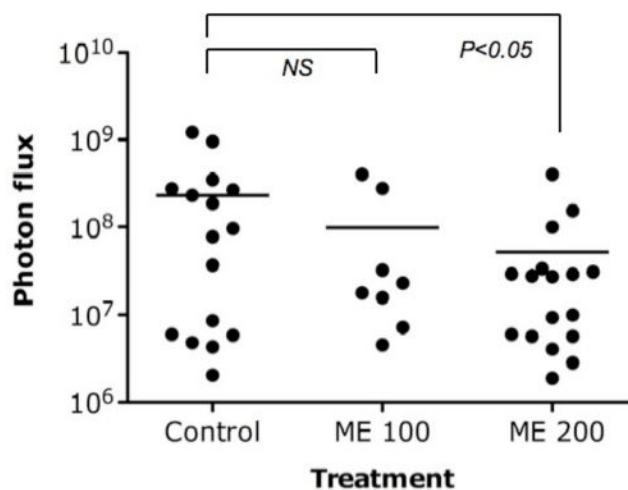
Figure 5.

Kaplan-Meier survival curves of MDA231 tumor-bearing mice treated with high or low doses of ME (2) or PBS begun at the time of tumor transplantation. NOD/SCID mice injected with MDA231 cells and treated three times per week with 40 mg/kg ME (2) begun at the time of tumor engraftment (ME post) or following resection of primary tumor at 2 weeks post engraftment (ME pre). * $P=0.005$. P-values were obtained using the log-rank test.

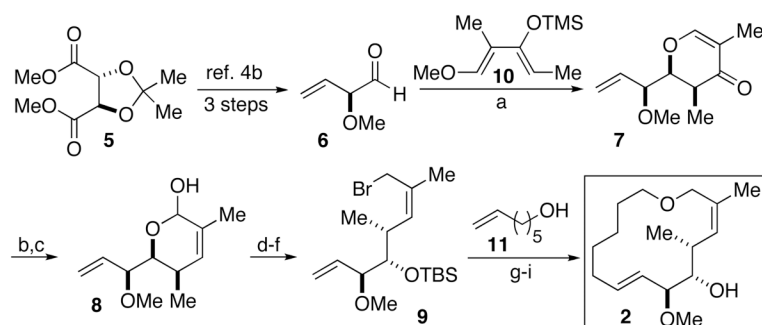
A.



B.

**Figure 6.**

Analysis of mammary tumor growth and lung metastasis. (A) Mammary tumor growth. Luciferase transduced LM2 cells were injected bilaterally into the fourth mammary gland fat pad of NOD.SCID mice. Size of the mammary tumor was measured regularly using a caliper. Day 27 after injection, mice underwent treatment with ME 100mg/kg, ME 200mg/kg or vehicle as control. The treatment was administered three times per week via intraperitoneal injection. Control: n=16, ME 100mg/kg: n=8, ME 200mg/kg: n=17. (B) Lung metastasis at endpoint measured by luminescence. At day 42, mice were analyzed for lung metastasis by ex vivo bioluminescence, quantifying luciferase activity in the lungs. NS: not statistically significant. ME 100: ME 100mg/kg, ME 200: ME 200mg/kg. P-values were determined using two-tailed Student's t-test.

**Scheme 1.**

Synthesis of Migrastatin Core Ether **2**.^a

^aKey: (a) (1) **10**, TiCl₄, DCM, -78 °C; (2) TFA, DCM; 87%; (b) LiBH₄, MeOH, THF, -10 °C; (c) CSA, H₂O, THF, reflux; (d) LiBH₄, MeOH, THF; 73%, 3 steps; (e) PPh₃, CBr₄, CH₃CN, 2,6-lutidine, rt, 85%; (f) TBSOTf, 2,6-lutidine, DCM, -15 °C, 91%; (g) **11**, NaH, THF, TBAI, 0 °C to rt; 90%; (h) Grubbs-II cat. 20%, toluene, reflux; 75%; (i) HF·Py, THF, 0 °C-rt, 90%.

Table 1Inhibition of transwell cancer cell migration by migrastatin ether (ME, **2**) and migrastatin ketone (MK, **4**).^a

| Cell Type | Cell Line | ME (2) IC ₅₀ (μM) | MK (4) IC ₅₀ (μM) |
|----------------------------------|------------|--|--|
| Breast Ca (mouse) | 4T1 | 0.47 ± 0.10 | n.d. |
| Breast Ca (human) | MDA-MB-231 | 0.30 ± 0.11 | n.d. |
| Breast Ca (human) | MDA-MB-435 | 0.37 ± 0.18 | 0.10 |
| Breast Epithelium Normal (human) | MCF10A | 408 ± 80 | n.d. |

^a Chemotaxis in response to a fetal calf serum gradient was measured after 12hrs in 6×24mm Transwell® (Corning) with 8.0μm pore size membrane inserts. Tumor cell migration was determined by counting cell attached to the underside of the membrane. ME or MK were added at 0 hrs to both upper and lower chambers over 5 log dilutions (1 nM, 10 nM, 100 nM, 1μM, 10 μM) with 3 wells at each dose. Data shown as half maximal inhibitory concentration (IC₅₀) in micromoles/L (μM). n.d: not determined.